Manipulating light at subwavelength scale by exploiting defect-guided spoof plasmon modes

A. Ourir,[1] A. Maurel,[1] S. Félix,[2] J.-F. Mercier,[3] and M. Fink[1]
[1]*Institut Langevin, ESPCI Paris, PSL, CNRS UMR 7587, 1 rue Jussieu, 75005 Paris, France*
[2]*Laboratoire d'Acoustique de l'Université du Maine, UMR CNRS 6613, Avenue Olivier Messiaen, 72085 Le Mans, France*
[3]*Poems, CNRS, ENSTA ParisTech, INRIA, 828 boulevard des Marchaux, 91762 Palaiseau, France*
(Received 13 October 2016; revised manuscript received 29 June 2017; published 19 September 2017)

We study the defect-guided modes supported by a set of metallic rods structured at the subwavelength scale. Following the idea of photonic crystal waveguide, we show that spoof plasmon surface waves can be manipulated at subwavelength scale. We demonstrate that these waves can propagate without leakage along a row of rods having a different length than the surrounding medium and we provide the corresponding dispersion relation. The principle of this subwavelength colored guide is validated experimentally. This allows us to propose the design of a wavelength demultiplexer whose efficiency is illustrated in the microwave regime.

DOI: 10.1103/PhysRevB.96.125133

I. INTRODUCTION

It is known that periodic structures can be designed in order to forbid the wave propagation in a desired frequency range. Based on this principle, waveguides in planar photonic crystals have been realized. They are obtained by changing the local properties of a periodic lattice along a channel, or waveguide, for instance by omitting one row of holes in a lattice of holes or by changing the hole size in one row [1–3]. In a surrounding medium where the propagation is forbidden, these waveguides support the propagation of so-called defect-guided modes. The guiding effect is particularly efficient when the wave number of the guided mode is below the light line since the mode propagates without leakage, being evanescent in the air above the guide. A similar guiding effect can be obtained in a material being structured periodically at the subwavelength scale. This has been done for electromagnetic waves using a set of metallic rods and reducing the length of a row of them [4]; interestingly in this case, the guided mode is a spoof plasmon (SP) mode supported by a waveguide with subwavelength width. Artificial structured materials have been notably proposed to produce spoof plasmons which masquerade at tera-Hertz and microwave frequencies as surface plasmons, these latter being limited to the visible range [5,6]. Their range of applications cover many wave guiding and focusing problems [7–11]. Theoretically, the condition for the spoof plasmon to take place is often interpreted as cavity resonances for a hole perforated massive media or as wire type resonances for very sparse structure. This argument predicts spoof plasmon working at frequencies correspondingly roughly to $L = \lambda/2$ or $L = \lambda/4$, with L the thickness of the structured material (Fig. 1). A more accurate dispersion relation of the spoof plasmons can be obtained by considering the propagation in an equivalent anisotropic material [12]. Within this description, spoof plasmons are waves being trapped within the artificial material, allowing for resonances tuned by the properties of the unit cell.

Wavelength-division multiplexing (WDM) allows us to expand the capacity of telecommunication systems without laying more channels [13]. Such systems use a demultiplexer at the receiver to separate the multiwavelength signal back into individual data signals and output them on separate channels. In this paper we use the principle of defect-guided modes in an artificial structured metamaterial supporting spoof plasmon waves to propose a wavelength demultiplexer. The device is able to drive an harmonic signal toward different channels at subwavelength scale. We start by analyzing the dispersion relation of a single waveguide. The guided modes is shown to be well described by a dispersion relation close to the dispersion of spoof plasmons but modified by the width of the waveguide. We start with the two-dimensional homogenized problem which yields the dispersion relation of classical spoof plasmons [12], and we extend to a three-dimensional problem. This principle is being validated experimentally, the design of the multichannel demultiplexer is proposed in order to avoid any overlapping in the dispersion relations of the different channels and its efficiency is demonstrated experimentally.

II. DISPERSION RELATION OF THE DEFECT-GUIDED MODES

Let us start with the classical spoof plasmon in a 1D array of layers (Fig. 1). Using an approximate modal method [5,6], the dispersion relation $\beta(k)$ (with β the wave number of spoof plasmons and k those of the free space) reads

$$\beta^2 = k^2[1 + \varphi^2 \tan^2 kL], \quad \tan kL > 0, \tag{1}$$

with φ the filling fraction of air and L the length of the layers.

In the framework of homogenization, this dispersion relation is recovered simply as the dispersion relation of a guided wave at the interface between the air and a homogenized medium described by the wave equation

$$\frac{\partial^2}{\partial z^2} H + k^2 H = 0, \tag{2}$$

and the associated conditions of continuity for H and $\varphi \partial_n H$ at the interface with the air [12]. Basically, the wave equation (2) tells us that the wave inside the grooves can only propagate along one direction (the z direction); it is worth noting that (2) does not imply that H is independent on (x, y); specifically, the solution is written

$$\begin{aligned} H &= e^{i\beta x} \frac{\cos kz}{\cos kL}, \quad 0 < z < L, \\ H &= e^{i\beta x} e^{-\sqrt{\beta^2 - k^2} z}, \quad z > L, \end{aligned} \tag{3}$$

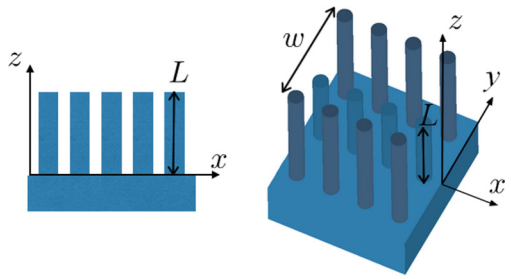

FIG. 1. 2D geometry of metallic layers between a ground plane and the air, spoof plasmons can propagate according to (1) [Left side]. 3D geometry of a structured waveguide of width w, guided modes can propagate according to Eq. (6) [Right side].

and this form of the solution ensures that H is continuous and that the Neumann boundary condition applies at the ground plane $\partial_z H(z=0)=0$. The last boundary condition $\varphi\partial_z H(L^-)=\partial_z H(L^+)$ at the interface with the air yields the dispersion relation (1), and the guided wave requires that $\beta > k$, which implies the additional constraint $\tan kL > 0$ in the dispersion relation; this latter condition defines the band gap. While in principle the upper frequency f_c^+ of the band gap is obtained for $kL=\pi/2$, from (1), it is in practice limited by the first Brillouin zone $\beta=\pi/a$, where

$$f_c^+\sqrt{1+\varphi^2\tan^2\frac{2\pi L f_c^+}{c}}=\frac{c}{2a},\quad f_c^+<\frac{c}{4L}. \tag{4}$$

To go toward our waveguide, we need to extend our model to a structuration in the y direction (Fig. 1). Thus, the 2D grooves are replaced by 3D rods with the same structuration along x and y. Following Ref. [5], this is expected to produce an equivalent transverse isotropic medium, with the axis of anisotropy along z; thus, the wave equation (2) should remain valid and we assume that φ can be simply replaced by the volume fraction of air in the rods; with cylindrical rods of radius r, we use $\varphi=1-\pi r^2/a^2$. Next, we extend the homogenization result to this 3D configuration looking for a solution of the form

$$\begin{aligned} H &= e^{i\beta x}\frac{\cos kz}{\cos kL}\cos\left(\frac{\pi y}{w}\right),\quad 0<z<L,\\ H &= e^{i\beta x}e^{-\sqrt{\beta^2+(\pi/w)^2-k^2}z}\cos\left(\frac{\pi y}{w}\right),\quad z>L. \end{aligned} \tag{5}$$

In the simple form thought above, we added a dependence in the y direction which accounts for Neumann boundary conditions at $y=0,w$, thus reducing the effect of the long rods surrounding the waveguide to those of metallic plates where the electric field vanishes. Otherwise, (5) accounts for the continuity of H at the interface with the air and for the Neumann boundary condition at the ground plane; as shown previously, the additional condition $\varphi\partial_z H(L^-)=\partial_z H(L^+)$ yields the new dispersion relation

$$\beta^2=k^2[1+\varphi^2\tan^2 kL]-\left(\frac{\pi}{w}\right)^2. \tag{6}$$

In (6), the band gap above f_c^+ still exists, and it does not significantly differ from (4) (it is sufficient to replace $1/a$ by $\sqrt{a^{-2}+w^{-2}}$); but now, a new band gap has appeared below the cut-off frequency f_c^- [given from (6) for $k\tan kL=\pi/(w\varphi)$].

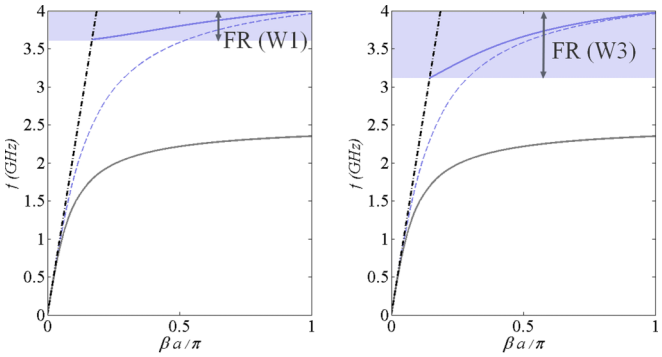

FIG. 2. Theoretical dispersion relations of the guided modes, Eq. (6), in plain blue lines for the W1 and W3 guides (see text), respectively, in (a) and (b), defining the frequency range FR (blue colored areas) where guided modes can propagate without leakage. The gray and the dashed black curves show, respectively, the dispersion relation of the surrounding medium and the light line. For comparison, dotted blue lines report the behavior of the classical spoof plasmons, Eq. (1).

The existence of the resulting finite pass band operating in the frequency range $[f_c^-,f_c^+]$ is the key to realize the desired filter; in the following, we denote FR(waveguide) $=[f_c^-,f_c^+]$ this frequency range:

$$f_c^-\tan\frac{2\pi f_c^-}{c}=\frac{c}{2w\varphi}. \tag{7}$$

Note that a third region with $\beta^2<0$ has appeared for frequencies below f_c^+ and above f such that $\beta(f)=0$ in (6); this corresponds to waves propagating in the waveguide but radiating in the air above the waveguide.

Figure 2 reports the dispersion relations (1) and (6) in two configurations. In the first one, referred to as the W1 guide, we use a surrounding medium, called gray medium $L_s=30$ mm and $a=7$ mm; the guide is created by reducing the length of a unique row of rods, where $w=2a=14$ mm, to $L=17$ mm; in the second configuration, the guide is created in a similar gray medium by reducing the length of three rows, where $w=4a=28$ mm, to $L=17$ mm. In the two configurations, the propagation is forbidden in the gray region when operating at a frequency in the finite pass bands of the waveguides, namely FR(W1) = [3.65–4] GHz and FR(W3) = [3.15–4] GHz.

III. NUMERICAL AND EXPERIMENTAL VALIDATION

To begin with, we validate numerically and experimentally the existence of the pass band rf, and check the validity of our predictions of the bounds f_c^+ and f_c^- in (4) and (7) and of the associated wave number (6). Experimental prototypes of the W1 and W3 waveguides have been realized. Measurements in the range [2.1–4] GHz have been performed in a semi-anechoic chamber using an Agilent 8722ES network analyzer. An S-band coaxial-to-waveguide transition has been used as an excitation source. An electric near-field probe mounted on a motorized two-dimensional scanning system is used to measure the field distribution at a distance of about 1 mm above the structure. A transmission coefficient has been also

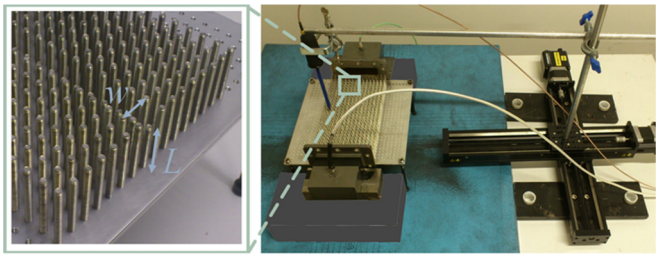

(a)

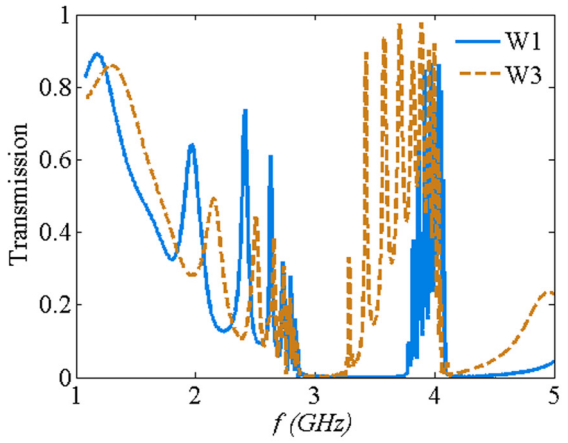

(b)

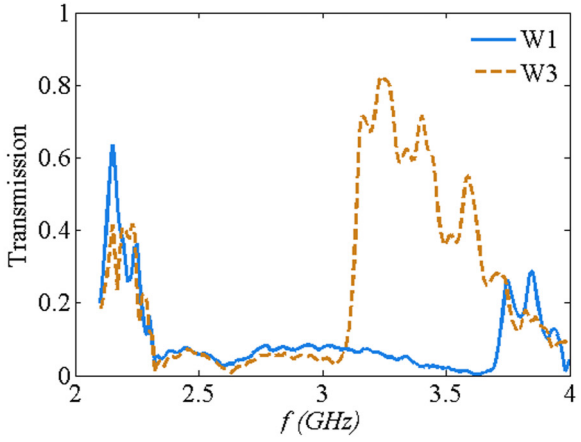

(c)

FIG. 3. (a) Photography of the experimental setup designed for the microwave range. A zoom on a W1 waveguide is presented on the right side. Simulated (b) and measured (c) transmission spectra of the W1 and W3 channels as a function of the frequency.

evaluated by placing a second coaxial-to-waveguide transition at the end of the artificial waveguide and by implementing a normalization to the free air transmission between the emitter and the receptor. Additional information on the experimental setup is given in the Supplemental Material [14].

First, we report in Fig. 3 the transmission in the channel as a function of the frequency. In both cases, the existence of a finite pass band is confirmed. These transmission bands correspond to the defect modes predicted in the theoretical dispersion relation (blue curves in Fig. 2). The obtained waveguides are called colored. The numerical calculations show good agreement with the corresponding experimental

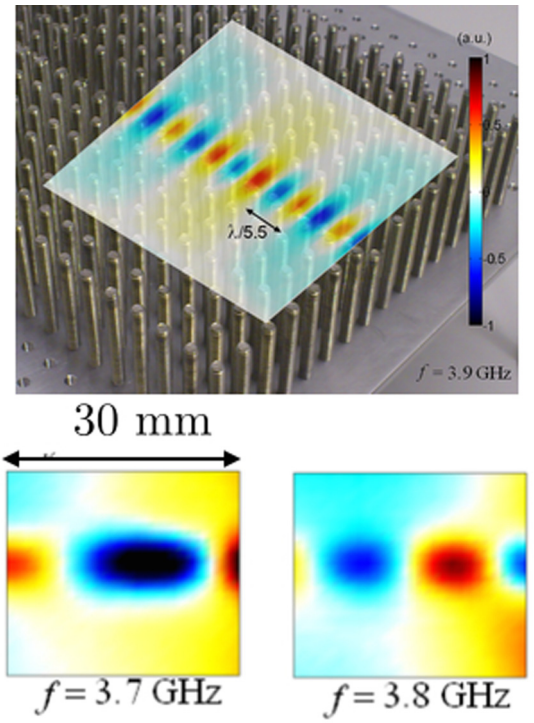

FIG. 4. Typical fields measured just above the rods in the colored guide W1.

results. Besides, the observed bounds of the FR are in good agreement with the theoretical predictions presented previously. One can notice here the importance of the attenuation for the spoof plasmon modes providing the smallest wavelengths. These wavelengths correspond to the highest frequencies in the transmission bands. This phenomenon, known in plasmonics, happen due to intrinsic losses in the considered materials for the high-wave-vector components. Additional results and discussions are provided in the Supplemental Material [14].

Figure 4 reports typical fields measured just above the rods in the colored waveguide W1 (same measurements, not reported, have been done for the W3 waveguide). This result shows the subwavelength propagation obtained in the proposed waveguides. The higher the frequency, the smaller is the wavelength λ_{GM} of the guided modes. From such measurements, the wavelength λ_{GM} can be estimated.

Below, quantitative results are collected for the W1 guide and compared to the prediction given by the dispersion relation (6) (see also Fig. 2).

W1 guide ($w = 2a$, $L = 17$ mm):

f (GHz)	3.7	3.8	3.9
measured λ_{GM} (mm)	42	30	21
$\lambda_{GM} = 2\pi/\beta$ from (6)	43	28	20

(8)

Again, the agreement between the measurements and the prediction of (6) is very good.

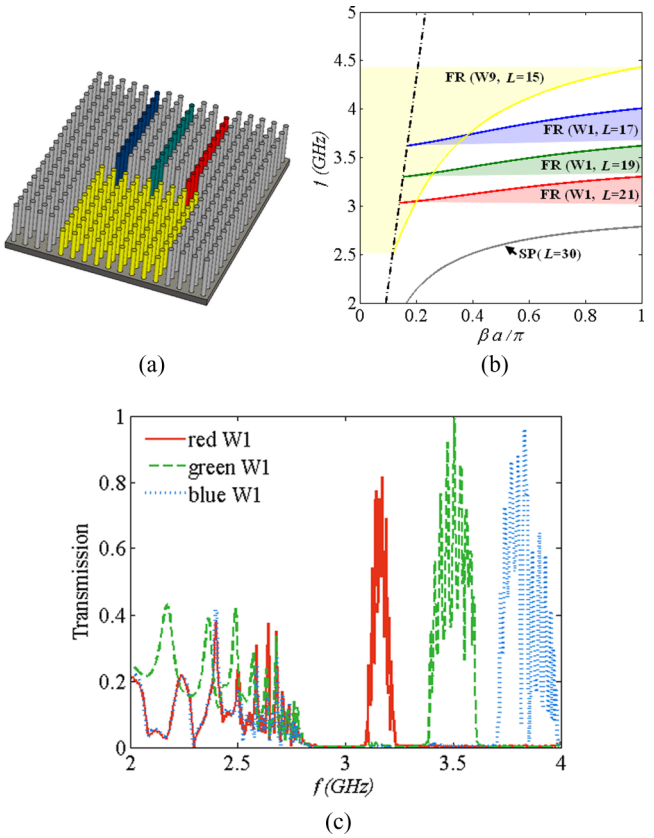

FIG. 5. (a) Schematic view of the multichannel demultiplexing device operating at subwavelength scale. (b) Dispersion relations of the four colored waveguides. The dispersion relation of the surrounded medium and the light line are also plotted for comparison in gray and dashed black, respectively. (c) Transmission spectra calculated at the exits of the three colored W1 waveguides.

IV. DEMULTIPLEXING BY EXPLOITING EFECT GUIDED SPOOF-PLASMON MODES

Since this validation is being performed, we move to the multichannel demultiplexer. The principle of the demultiplexing is shown in Fig. 5. A main waveguide, called white guide, is built in order that the FR(white) covers the working frequency range; this is done by choosing (i) w large enough to produce a small enough f_c^- [see (7)] and (ii) L small enough to produce a large enough f_c^+ [see (4)]. By setting $w = 10a = 70$ mm and $L = 15$ mm, we expect FR(white) $= [2.5; 4.5]$ GHz.

Next, three colored waveguides (red, green, blue) are designed in order to support guided mode propagation in three different frequency ranges with no overlapping. Again from (4) and (7), thin FR are obtained for small w and we set $w = a = 7$ mm. By choosing $L = 17$, 19, and 21 mm, we expect this condition to be fulfilled with

$$\begin{aligned} &\text{FR(red)} = [3; 3.3], \quad \text{FR(green)} = [3.3; 3.6], \\ &\text{FR(blue)} = [3.6; 4.0]. \end{aligned} \tag{9}$$

Full wave numerical simulations have been performed for the proposed multichannel demultiplexer. Figure 5(c) shows the transmission spectra calculated at the exits of the three W1 waveguides. Three transmission bands are obtained at the specific frequency bands predicted by the dispersion relations.

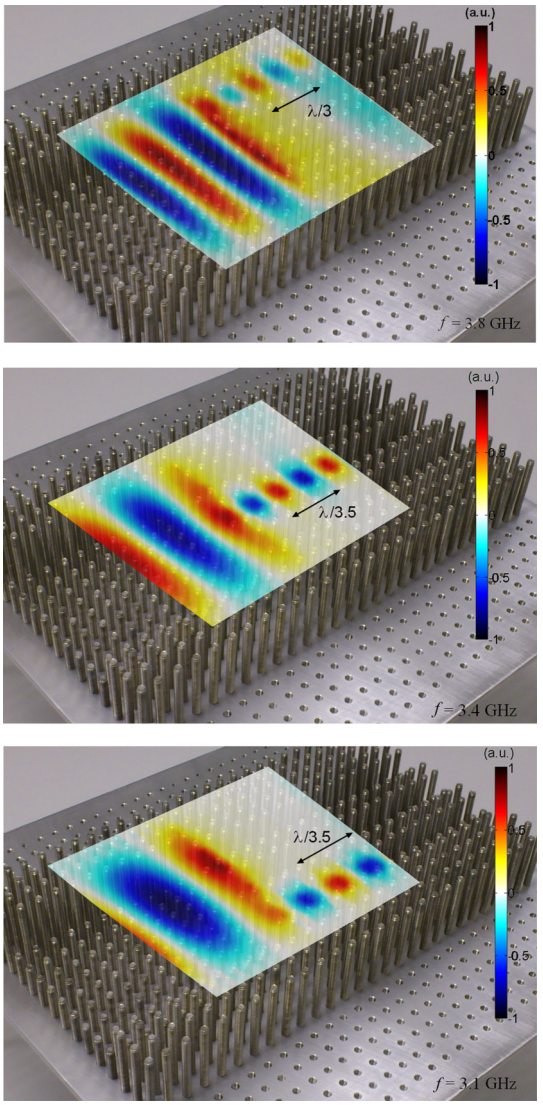

FIG. 6. Electric fields scanned above the structure at three frequencies chosen, respectively, in the red ($f = 3:1$ GHz), green ($f = 3:4$ GHz), and blue ($f = 3:8$ GHz) frequency range $[fc-; fc+]$.

The efficiency of the demultiplexer has been tested experimentally and it is illustrated in Fig. 6. The white guide is able to support the wave propagation in the whole range of our working frequency; next, the demultiplexing efficiently directs the signal into single colored waveguides, accordingly to the predicted FR.

V. CONCLUSIONS

We have presented the principle of manipulating light at subwavelength scale by exploiting defect-guided spoof plasmon modes. We have shown that such modes are supported by a set of metallic rod structures at subwavelength scale. We have proposed a multichannel demultiplexer based on the existence of spoof plasmon guided modes being supported within a finite pass band, with upper and lower bounds. The multichannel demultiplexer is based on the behavior of a single waveguide supporting spoof plasmon modes for which the

dispersion relation has been obtained. Each waveguide consists of a structured material able to produce plasmonic propagation at subwavelength scale that can be tuned with high flexibility. Such devices can be exploited in rf telecommunications for demultiplexing a number of carrier signals. This approach could be extended to infrared and optics to be used in WDM fiber communications.

In terms of theoretical extension, a more accurate model could be proposed. As presented in this paper, the model starts from a homogenization approach valid for a two-dimensional structuration and that we extended to a three-dimensional structuration within several approximations. Although our approach allows for a simple expression, a more accurate model should consider the 3D homogenization of the waveguide in the surrounding medium.

ACKNOWLEDGMENTS

This work is supported by LABEX WIFI (Laboratory of Excellence within the French Program "Investments for the Future") under references ANR-10-LABX-24 and ANR-10-IDEX-0001-02 PSL*.

[1] A. Mekis, J. C. Chen, I. Kurland, S. Fan, P. R. Villeneuve, and J. D. Joannopoulos, Phys. Rev. Lett. **77**, 3787 (1996).

[2] A. Chutinan and S. Noda, Phys. Rev. B **62**, 4488 (2000).

[3] S. Kuchinsky, D. Allan, N. Borrelli, and J.-C. Cotteverte, Opt. Commun. **175**, 147 (2000).

[4] F. Lemoult, N. Kaina, M. Fink, and G. Lerosey, Nat. Phys. **9**, 55 (2013).

[5] J. B. Pendry, L. Martn-Moreno, and F. J. Garcia-Vidal, Science **305**, 847 (2004).

[6] F. J. Garcia-Vidal, L. Martn-Moreno, and J. B. Pendry, J. Opt. A **7**, S97 (2005).

[7] S. A. Maier, S. R. Andrews, L. Martin-Moreno, and F. J. Garcia-Vidal, Phys. Rev. Lett. **97**, 176805 (2006).

[8] A. I. Fernandez-Dominguez, E. Moreno, L. Martin-Moreno, and F. J. Garcia-Vidal, Phys. Rev. B **79**, 233104 (2009).

[9] D. Martin-Cano, M. L. Nesterov, A. I. Fernandez-Dominguez, F. J. Garcia-Vidal, L. Martin-Moreno, and E. Moreno, Opt. Express **18**, 754 (2010).

[10] S.-H. Kim, T.-T. Kim, S. Oh, J.-E. Kim, H. Park, and C.-S. Kee, Phys. Rev. B **83**, 165109 (2011).

[11] Y. Xiao, M. Klein, M. Hohensee, L. Jiang, D. F. Phillips, M. D. Lukin, and R. L. Walsworth, Phys. Rev. Lett. **101**, 043601 (2008).

[12] J.-F. Mercier, M. L. Cordero, S. Félix, A. Ourir, and A. Maurel, Proc. R. Soc. London Sect. A **471**, 2182 (2015).

[13] W. J. Tomlinson, and C. Lin, Electron. Lett. **14**, 345 (1978).

[14] See the Supplemental Material at http://link.aps.org/supplemental/10.1103/PhysRevB.96.125133, which includes Refs. [6,15], for additional information on the homogenization approach and technical descriptions of the full wave simulations and the microwave experiments presented in the main paper.

[15] E. J. Zeman and G. C. Schatz, J. Phys. Chem. **91**, 634 (1987).